ADJUSTABLE SUBREFLECTOR MECHANISM

Carlos Compostizo[(1)], Jose Maria Arroyo[(1)], Lucio Scolamiero[(2)]

[(1)]*SENER, Avda Zugazarte 56, 48930 Las Arenas (SPAIN), carlos.compostizo@sener.es ; jm.arroyo@sener.es ;*
[(2)] ESA, Noordwijk, (The Netherlands), Lucio.Scolamiero@esa.int

ABSTRACT

The paper presents the mechanisms developed in ESA TRP Contract Nº18186/04/NL/CH devoted to the development of the pointing technologies for the next generation of high frequency (Q/V frequency bands) antenna systems. The study was focused in the development of an adjustable subreflector as part of a hybrid mechanical-electronic pointing system. A dual con-focal Gregorian antenna system with a planar phase array was selected as the baseline system for the definition of the subreflector requirements. The hybrid pointing is achieved by means of the electronic steering provided by the phase array besides of the mechanically corrections achieved by the adjustable subreflector. The position and shape of the subreflector are mechanically adjusted to correct aberrations resulted during electrical beam scanning

The study dealt with the design, manufacturing and testing of a Breadboard Model of the Subreflector Assembly that includes a deformable disk and the mechanisms needed to change shape, position and orientation of the subreflector surface during steering.
The functional tests of the breadboard model included the measurement of the reflector surface. RF performances of the Antenna System were analysed using the measured surface of the subreflector.

1 ANTENNA CONFIGURATION

A dual con-focal Gregorian antenna system configuration [1] with a planar phase array was selected for this development of the hybrid mechanical electronic pointing system. The hybrid pointing is achieved by means of the electronic steering provided by the phase array besides of the mechanical system able to change position and shape of the subreflector.

For each scanning condition, an Ideal Subreflector surface is obtained by Geometrical Optics shaping techniques. Each ideal subreflector surface was approximated by the best fit paraboloid using least squares technique. Only three degrees of freedom of the paraboloid parameters were used for the best fit approximation; tilting angles (u,v) and focal length (f). Focus position (xF, yF, zF) has been made dependent of (u,v,f) parameters. The dependence is mechanically defined to fit with the focus position obtained when an unrestricted approximation is computed.
A Gregorian Antenna configuration was defined for the study with the following main characteristics. Main reflector aperture (D) is 960 mm and a focal length (f) of 1200 mm, whereas sub reflector aperture diameter is 676 mm (*DS)* with a focal length (*fs)* of 500 mm. The Fig.1 shows a diagram of Con-Focal Gregorian Antenna system with the phase array.

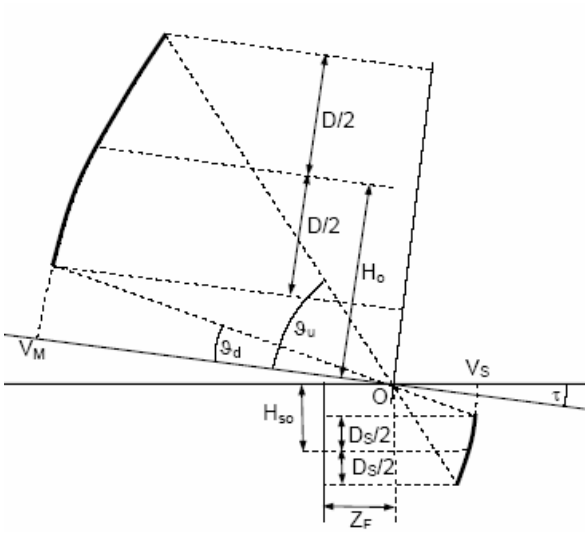

Figure 1. Con-focal Gregorian Antenna System

The required Subreflector Mechanisms adjustment capabilities for a beam scanning of +/-4º are defined by the paraboloid parameters for each beam scan angle. The strokes of the corrections are:

- Adjustment of focal length from 500 to 486mm.
- Translation of focus up to (-11;0;16)mm
- Reflector U Rotation around Y axis up to 0,012 rad=0,69º
- Reflector V Rotation around X axis up to ±0,003 rad=±0,19º

Proc. '12th Euro. Space Mechanisms & Tribology Symp. (ESMATS)', Liverpool, UK, 19–21 September 2007 (ESA SP-653, August 2007)

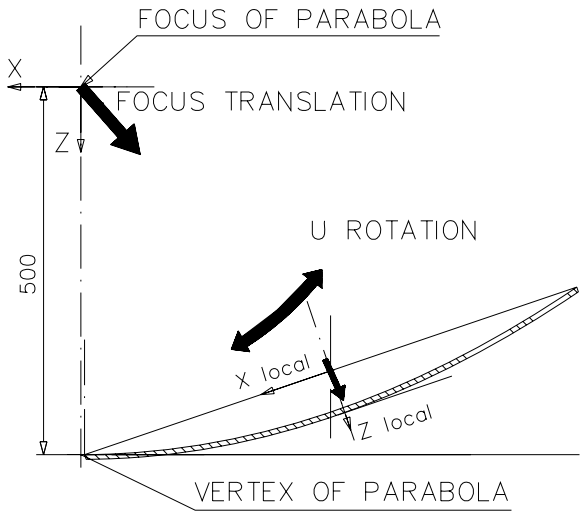

Figure 2. Subreflector reference Axis

The above adjustments requires the following displacements of central point (defined in local system)

- XL direction translation stroke from 0 mm to -8mm.
- YL direction translation stroke from -2.5 mm to 2.5mm
- ZL direction translation stroke from 0 mm to 2.5mm

2 SUBREFLECTOR ASSEMBLY DESIGN

The Subreflector Assembly includes a parabolic shape disk mounted on a structure which includes four flexible supports which allow the roto-translation and shape adjustment of the reflector by means of a set of mechanisms.
A hold down and release mechanism is required for the fixation of the sub reflector and the off-loading of the mechanisms and flexible supports during launch.

Figure 3. SubReflector Assembly configuration

2.1 Subreflector plate

The subreflector plate is a parabolic shape sandwich panel, with a honeycomb core and two fiber reinforced skins as thin as possible in order to allow its deformation for changing its curvature and hence focal length of the parabolic surface with minimum forces. Fig. 4 shows the subreflector after curing process.
The plate is manufactured with the nominal reflector shape for a 500 mm focal length paraboloid. For changing its focal length, the subreflector plate is pulled from its center through the inner interface ring and supported at its perimeter by means of sixteen outer supports studs. (See Fig. 5)

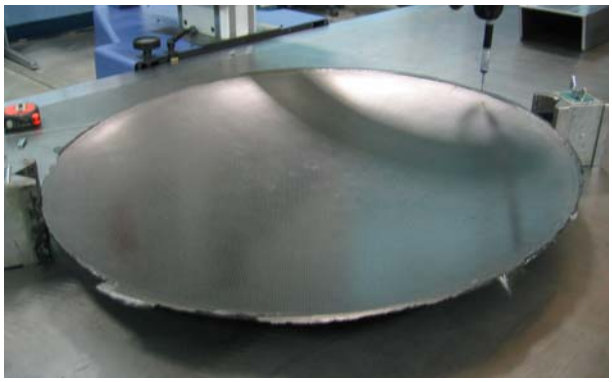

Figure 4. Subreflector plate just after curing

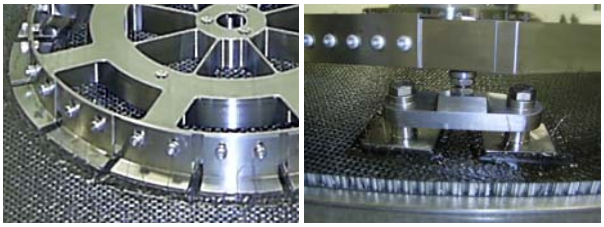

Figure 5. Subreflector plate bonding to inner and outer ring

2.2 Support Structures

The sub-reflector plate is uniformly supported in its periphery by means of sixteen bonding studs. Each pair of bonding studs is mounted on an octagonal ring via small brackets. The octagonal ring is mounted on four flexible supports, which work as guides allowing the required rigid body roto-translations of the subreflector.

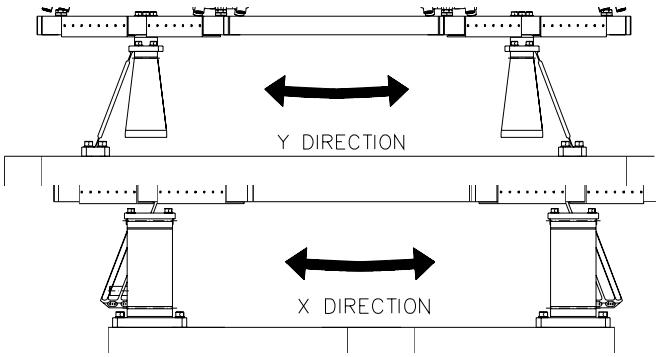

Figure 6. Outer Ring Support structure and flexible supports

The subreflector is also joined to a inner ring wheel by means of sixteen studs. The number of these studs has been defined in order to adjust the internal ring to the paraboloid shape. Slotted holes in screwed joint between studs and wheel allow the adjustments of the height for its proper bonding to the parabolic shape. The T section studs allow the uniform distribution of the forces generated by the actuation mechanism to the subreflector plate.

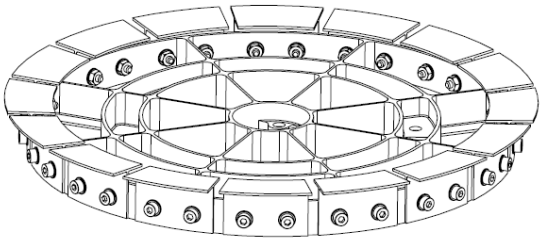

Figure 7. Inner ring Wheel and studs configuration

2.3 Hold Down and Release Mechanism

The Subreflector Hold Down and Release mechanism (HRM) is required to offload the adjustment mechanisms of the subreflector assembly during launch. It includes a central hold down made by three cup and cone pairs of pieces preloaded by a M8 bolt released by a pyronut and two lateral hold downs. These lateral hold downs are needed to increase the first eigen frequency due to a torsional vertical mode

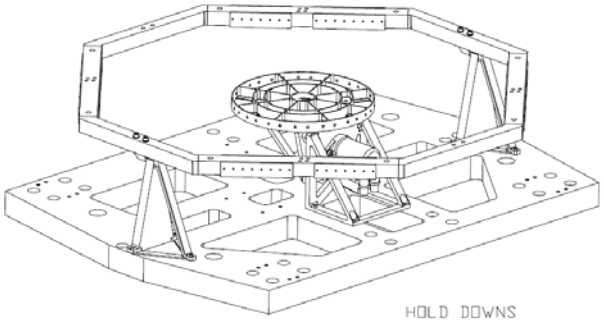

Figure 8. Hold Down and Release Mechanism Assembly

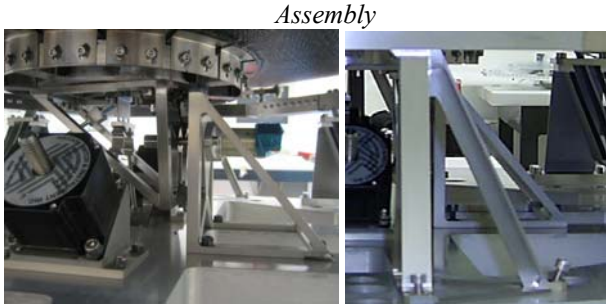

Figure 9. Central and lateral Hold Downs

2.4 Subreflector Adjustment Mechanisms

The subreflector mechanism shall be able to position, point and adjust the subreflector surface as required to optimize gain and correct aberrations. This objective is achieved by providing three translational degrees of freedom.

These subreflector adjustments are achieved by the displacement of the centre of the subreflector plate pulling through an inner ring by means three linear actuators. The three linear actuators built up by a stepper motor with an integrated nut and a spindle, are joined to the centre ring by flexible transmission components. This flexible transmission provides the reduction ratio to optimise the size of the actuators.

The use of flexible components instead of plain and spherical bearings allowed to remove the need of lubrication outside the motor bearings and spindle making that the transmission is not sensitive to the extreme temperatures the sub reflector will be exposed.

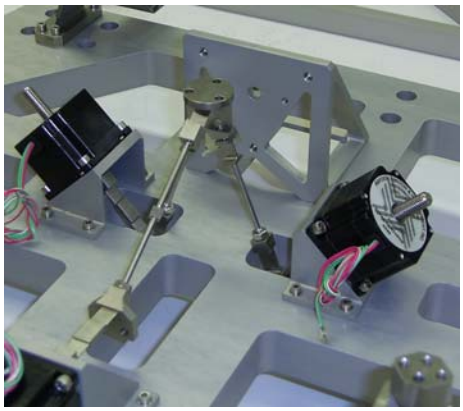

Figure 10. Isometric view of the Flexible Mechanisms

The focal length adjustment is achieved by pulling with a force up to 2700N in the +ZL direction by means of the two linear actuators (M2 & M3) of the YZ plane with the same displacements.

The +/-2.5mm displacements in the Y direction is provided by the differential displacements of the YZ plane actuators (M2 & M3). To reach the maximum Y displacement one of the motors in the YZ plane must impose a large displacement and the second a very small displacement but always positive. This makes all the elements remain working in tension with the exception of the actuator pushing rod.

Figure 11. YZ Actuators for displacements in z direction and in YZ plane

The (M1) actuator in the ZX plane provides a displacement of the subreflector up to 8 mm in the -X direction achieving the required U rotation and also helps to provide the Z vertical load required to deform the subreflector plate.

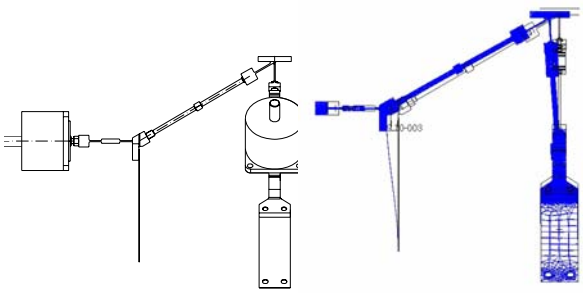

Figure 12. X actuator for X direction displacement

The geometry of the mechanism has been defined to provide maximum reduction ratio between the YZ plane actuators displacements and the Z displacement. Nevertheless, the X axis actuator with very small reduction ratio achieves the translation in the X direction. The displacement in the YZ plane actuators are 4,7 mm to achieve the Z displacement of 2.4 mm, while the displacement for the XZ plane actuator is 8.7mm to achieve a X displacement of 7.6 mm.

3 ADJUSTABLE SUBREFLECTOR MECHANISM TESTING

3.1 Vibration Tests

The adjustable subreflector was subjected to sinusoidal and Random vibration Test in order to verify its structural integrity. In particular the objectives were to prove its capability to survive to the expected dynamic environment, to verify the resonant frequencies calculated by analysis and to confirm that the item was free from workmanship errors.
The assembly withstood the qualification level vibration tests. The first natural frequencies of the assembly was 103 Hz always above than the 80 Hz required.

Axes	Frequency (Hz)	Qualification Test Limits
X & Y & Z	5-21 21-60 60-100	11mm 0 to peak 20g 6g

Table 1. Sinusoidal Vibration Test Levels

Freq(Hz)	Levels
20 to 100	+3 dB/oct
100 to 300	0.5 g2/Hz
300 to 2000	-5 dB/oct
Grms	16.92 g
Duration	2,5 minute

Table 2. Random Vibration Test Levels

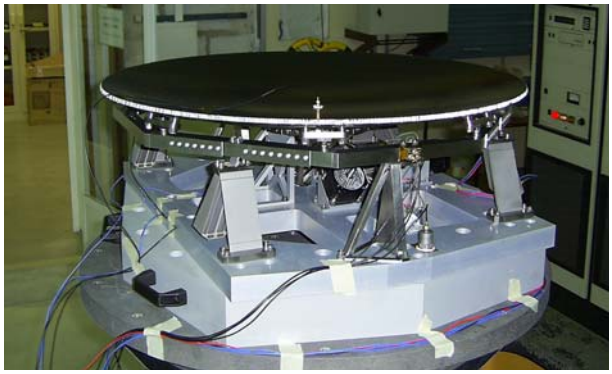

Figure 13. Subreflector Assembly Vibration Test

3.2 Functional Tests

The functional tests were performed in order to verify that the Adjustable subreflector mechanism was capable to position, point and adjust the sub-reflector surface as required.

The predictions of the mechanisms kinematics and dynamics were obtained by mean of a non linear structural analysis. This analysis allowed to predict the position of the subreflector surface derived from the actuators displacements. Using the calculated positions of the subreflector surface the best fit paraboloid parameters; focal length, position and orientation were calculated. Therefore the relationship between actuator displacements and sub reflector independent parameters (focal length, orientation angle U and V) was obtained. The relationship between focus position and the selected independent parameters was also obtained by this analysis.
The result of the analysis showed a non linear relationship which was calculated and approximated by a formulation which allowed us to derive motor positions for each independent set of sub reflector parameters which correspond to each scan angle. The following relationships are defined for the independent variables:

$$-0.29\cdot M_1-0.889\cdot M_2-0.889\cdot M_3+500-0.068\cdot M_1\cdot M_2 - -0.068\cdot M_1\cdot M_3 + 0.122\cdot M_2\cdot M_3 = \text{Focal Length} \quad (1)$$

$$-1.663\cdot M_1+0.166\cdot M_2+0.166\cdot M_3+0.024\cdot M_1\cdot M_2 + +0.024\cdot M_1\cdot M_3-0.053\cdot M_2\cdot M_3 = \text{U Angle} \quad (2)$$

$$-0.979\cdot M_2+0.979\cdot M_3-0.017\cdot M_1\cdot M_2+0.017\cdot M_1\cdot M_3=\text{V Angle} \quad (3)$$

Where
Mechanism variables: displacements [mm] of three motors (M_1, M_2, M_3).
Independent design variables: Focal Length, U and V angles.

Three sets of functional test were carried out in order to verify these equations.
The initial functional tests were carried out measuring displacements of the reflector with dial indicators (see Fig. 14). These initial tests confirmed the Adjustable subreflector mechanism movements of rigid solid adjusted to the trajectories predicted by analysis. These tests were repeated after vibration tests in order to verify no degradation of mechanism assembly.

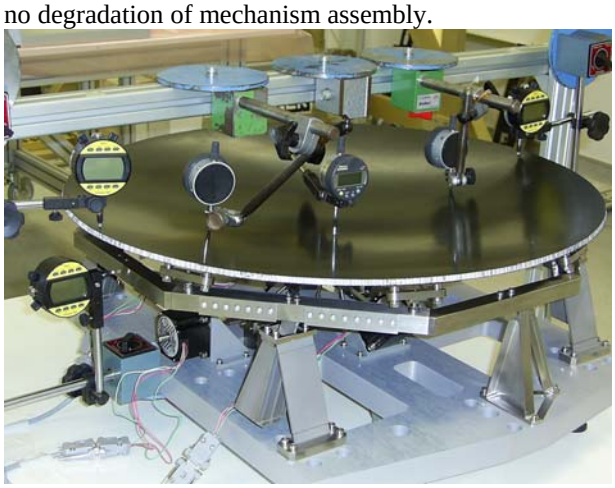

Figure 14. Dial gauges configuration for initial tests

The second tests were performed to verify the capability of Adjustable Subreflector mechanism to position, point and adjust the subreflector surface to the several extreme cases measuring the surface of the reflector at more than 1400 points. A 3D machine was used to obtain the adjusted sub reflector surface position for each functional case. Measured and analytically predicted surface was compared with the required paraboloid and RMS errors were calculated (see Fig. 16 and Table 3).

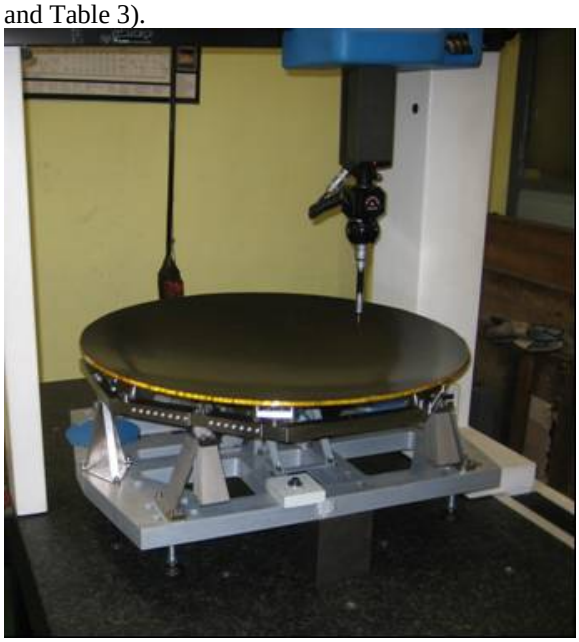

Figure 15. Shape Measurements during functional test

Case	**M1=0 M2=0 M3 = 0** (ϕ=0°,θ=0°)	**M1=8.64 M2=4.74 M3=4.74** (ϕ=0°,θ=5°)	**M1=7.84 M2=1.31 M3=4.27** (ϕ=76°, θ=4.12°)	**M1=1.31 M2=7.84 M3=4.27** (ϕ=284°, θ=4°)
Measured 3D	65	127	79	61
Calculated FEM	0	94	107	107

Table 3. Comparison between measured and calculated RMS error [μm] with respect to the required paraboloid.

The RMS errors of the measured shape were around 20% higher than the calculated shape with the non linear structural analysis. This is considered quite good knowing that measured values include the error of the manufactured reflector of 70 microns.

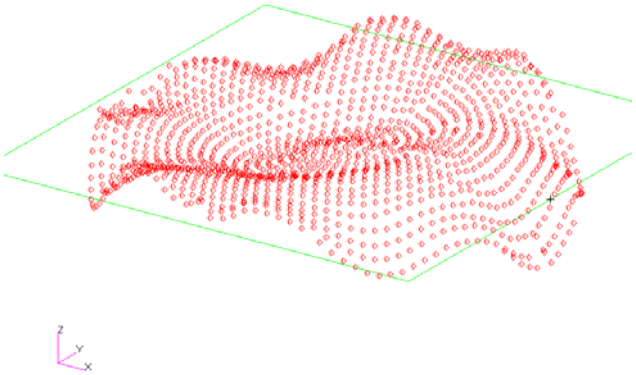

Figure 16. Errors between required paraboloid surface and measured position of sub reflector surface.

3.3 Life test

The capability of the mechanisms to withstand the expected number of adjustment cycles was also verified performing the following cycles :

- 2000 cycles defined by a stroke in the motors of (M1= 3.584, M2=M3= 1.865)corresponding to a scan angle of Phi= 0º and Theta = 3º
- 1000 cycles defined by a displacement of 8.638 for M1 and 1.865 for M2 and M3
- 8 cycles at maximum displacements of 8.638 for M1 and 4.704 for M2 and M3

4 RF Performances analysis

The Physical Optics (PO) analysis for calculation of the RF performances was also performed (see [1] & [2]). A planar aperture source at 50GHz is modelled. The induced currents across the subreflector are computed under PO approximation on a number of subreflector triangular patches generated from predicted and

measured surface points. Spill over and subreflector blockage effects are taken into account. The Physical Theory of Diffraction (PTD) is used to compute the effects of the surface rim. The computed gain results show very good correlation between the ideal surface MR-TBF cases, which is the target design, and the FEM predicted results and measured ones. In the worst case, the subreflector adjustment is able to recover a gain higher than 1.1 dB with respect to the nominal case. The Gain in all the field of view is equalized to differences under 0.3 dB for the simulations with the measured surfaces. Radiating patterns obtained with measured and ideal subreflector surfaces are very similar.

Computed Gain dB	Nominal	Ideal MR-TBF	FEM Simulated subreflector	Functional Tests Set #1	Functional Tests Set #2
ϕ=0°, θ=0°	53.42	------	------	53.42	53.41
ϕ=0°, θ=5°	51.98	53.20	53.08	53.14	53.15
ϕ=76°, θ=4.12°	52.67	53.18	53.12	53.13	53.12
ϕ=-76°, θ=4.12°	52.67	53.18	53.12	------	53.10

Table 4. Gain dB Summary Results

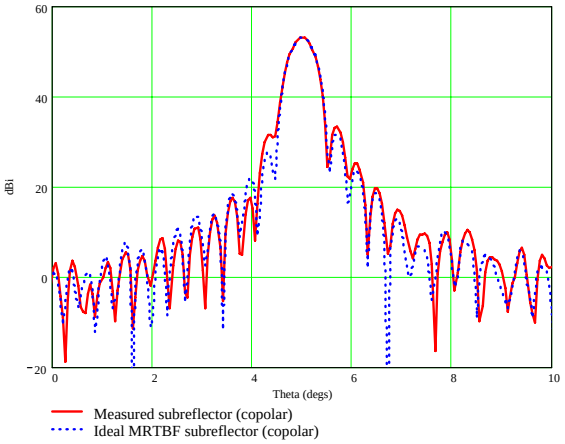

Figure 17. RF performances for the worst case

5 CONCLUSIONS

The conclusions of the study are:

- The feasibility of a hybrid electronic mechanical scanning system at 50 GHz has been demonstrated.
- Adjustable Subreflector Assembly concept have been designed, manufactured and tested.
- Satisfactory RF performances have been demonstrated by calculation of the gain recovery obtained with corrections provided by the Adjustable Subreflector.
- Focal length adjusting of the subreflector has been demonstrated feasible to improve Ku/Ka bands systems

6 REFERENCES

1. A.G. Pino, J.A. Martinez Lorenzo, A.M. Arias, J.O. Rubiños, J. Basterrechea, C. Compostizo, L. Scolamiero. “A Gregorian Confocal Reflector Antenna with Adjustable Subreflector for the Hybrid Mechanical-Electronic Pointing System at the Satellite Q/V Band”. IEEE AP-S International Symposium, Washington, July 2005.
2. J.A. Martinez, A.G. Pino, I. Vega, M. Arias and J.O. Rubiños. ICARA: Induced Current Analysis of Reflector Antennas. IEEE Antennas and Propagation Magazine. Vol.47 pp.92-100. April 2005